J Syst Sci Complex (2019) 32: 1358–1374

Robust Finite-Time Trajectory Tracking Control of Wheeled Mobile Robots with Parametric Uncertainties and Disturbances*

GUO Yijun · YU Li · XU Jianming

DOI: 10.1007/s11424-019-7235-z
Received: 10 July 2017 / Revised: 14 May 2018

Abstract In this paper, a robust finite-time tracking control scheme is proposed for wheeled mobile robots with parametric uncertainties and disturbances. To eliminate the effect of lumped uncertainties, a nonlinear extended state observer (NESO) is employed to estimate the unknown states as well as uncertainties, and the corresponding coefficients are tuned via pole placement technique. Based on the observation values, the finite-time sliding mode controller is presented to guarantee that both the sliding mode variables and tracking errors converge to zero within finite time. Simulation results are given to demonstrate the effectiveness of the proposed control method.

Keywords Finite-time sliding mode control, nonlinear extended state observer, trajectory tracking, wheeled mobile robot.

1 Introduction

Wheeled mobile robot (WMR) trajectory tracking control is not only an important issue in practical application but also an important research problem. However, due to the influence of the parametric uncertainties and external disturbances in the system, the robust tracking controller design is still a challenging task.

In order to enhance the robustness and the tracking control performance of the system, many kinds of control methods are applied to the control of the WMR. Such as adaptive control[1, 2], backstepping control[3, 4], sliding mode control[5–7], etc. In [2], a new adaptive controller is designed for tracking control of nonholonomic mobile robot with unknown slipping and external disturbances. In [3], to improve the tracking performance of the nonholonomic mobile robot

GUO Yijun · YU Li · XU Jianming
College of Information Engineering, Zhejiang University of Technology, Hangzhou 310023*, China.*
Email: 1121403105@zjut.edu.cn.
*This research was supported by the National Natural Science Foundation of China under Grant No. 61673351 and the Zhejiang Provincial Natural Science Foundation of China under Grant No. LZ15030003.
◇ *This paper was recommended for publication by Editor HU Xiaoming.*

trajectory tracking, a robust backstepping control method based on nonlinear disturbance observer is presented. The work of [5] presents a novel integral sliding mode controller for a two-wheeled mobile robot, the simulation and experiment results are provided to demonstrate the effectiveness of the work. Among these methods, the sliding mode control method is considered as an influential method to deal with nonlinear uncertain systems because of its strong robustness against uncertainties.

However, in traditional sliding mode control the sliding surface is linear, which will lead to the system states converge to origin in an infinite time. In order to improve the convergence rate of sliding mode control method, an efficient way is to introduce nonlinear sliding mode surfaces[8]. Terminal sliding surface is one of such nonlinear sliding surfaces, which can ensure that the system states can converge to zero in finite time[9, 10]. Another obvious problem in traditional sliding mode control is chattering, which will shorten the service life of actuator and even cause the system instability. To solve this problem, we will employ nonlinear extended state observer (NESO) to estimate the uncertainties of the system. As a kind of disturbance estimate technique, NESO regards the lumped uncertainties as a new state of the system, and the observed value can be further employed to compensate the uncertainties by feed-forward method[11–14]. By the feed-forward compensation, the switching gains of the sliding mode controller can take smaller values, which will obviously reduce chattering in the control signals.

In this paper, a robust finite-time controller is developed to improve the performance of tracking control and robustness against uncertainties for the WMR. Firstly, the model of the wheeled mobile robot with lumped disturbances is established at the dynamic level. Secondly, a nonlinear extended state observer is designed to estimate the uncertainties, then based on the estimation value a robust finite time trajectory tracking controller is developed. Finally, the simulation results are provided to verify the effectiveness of the proposed control scheme.

The main contributions are shown as follows:

1) A robust finite-time control law for trajectory tracking control of WMR is designed, which can guarantee that the system tracking errors converge to zero within finite time. The proposed control scheme is only depend on the nominal model of the system, thus it can be applied to the WMR system with lumped disturbances.

2) The excellent disturbance rejection performance is achieved by the estimation of NESO, and the parameters of the nonlinear extended state observer are determined by the pole placement technique, which greatly simplifies the parameter tuning process.

3) By compensating for the lumped disturbances of the system, the high gain problem of the controller can be avoided. Thus, the chattering phenomenon in the controller is weakened.

2 Problem Description

As shown in Figure 1, the mobile robot has two actuated wheels mounted on the same axis and a castor wheel to maintain the equilibrium of the WMR. The kinematic model[15] of the

WMR with the constraints of pure rolling and no slipping is described as

$$\dot{q} = J(q)u = \begin{bmatrix} \cos\theta & 0 \\ \sin\theta & 0 \\ 0 & 1 \end{bmatrix} \begin{bmatrix} v \\ \omega \end{bmatrix}, \tag{1}$$

where $q = [\ x \quad y \quad \theta\ ]^{\mathrm{T}} \in R^3$ denotes the position and orientation of the WMR; $u = [\ v \quad \omega\ ]^{\mathrm{T}} \in R^2$ is a vector consisting of the linear velocity and angular velocity.

According to the Euler-Lagrange formulation, the dynamic model[15] of the WMR is described as

$$M(q)\ddot{q} + C(q,\dot{q})\dot{q} + G(q) + F(\dot{q}) + \tau_d = B(q)\tau - A^{\mathrm{T}}(q)\lambda, \tag{2}$$

where

$$M(q) = \begin{bmatrix} m & 0 & 0 \\ 0 & m & 0 \\ 0 & 0 & I \end{bmatrix}, \quad B(q) = \frac{1}{r}\begin{bmatrix} \cos\theta & \cos\theta \\ \sin\theta & \sin\theta \\ b & -b \end{bmatrix}, \quad A^{\mathrm{T}}(q) = \begin{bmatrix} -\sin\theta \\ \cos\theta \\ 0 \end{bmatrix},$$

$\tau = [\tau_l\ \tau_r]^{\mathrm{T}}$, $\lambda = -m(\dot{x}\cos\theta + \dot{y}\sin\theta)\dot{\theta}$; m is the mass of the WMR; I is the inertia of the WMR; r and $2b$ are the radius of the driven wheel and the distance of the driven wheels; τ_l and τ_r are the control torques generated by the left driven wheel and the right driven wheel, respectively; λ is the Lagrange multiplier; The $F(\dot{q}) \in R^3$ is the unknown ground friction; $\tau_d \in R^3$ denotes the unknown bounded disturbance; $C(q,\dot{q})$ denotes the centripetal and coriolis matrix, $G(q)$ is the gravitational vector. Suppose that the center of mass of mobile robot is located in the middle of the rear wheel axis, and the mobile robot moves in the horizontal plane, then we can conclude that $C(\varphi,\dot{\varphi}) = G(\varphi) = 0$.

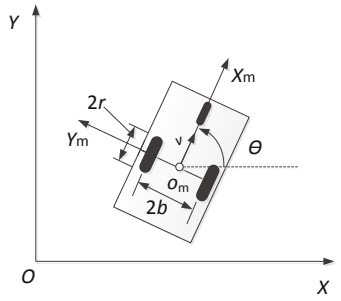

Figure 1 The platform of mobile robot

By multiplying $J^{\mathrm{T}}(q)$ on both sides of (2) and using the fact $J^{\mathrm{T}}(q)A^{\mathrm{T}}(q) = 0$, one can obtain the following dynamic model

$$\overline{M}\dot{u} + \overline{F} + \overline{\tau}_d = \overline{B}\tau, \tag{3}$$

where $\overline{M} = J^{\mathrm{T}}(q)MJ(q) \in R^{2\times 2}$, $\overline{F} = J^{\mathrm{T}}(q)F \in R^2$, $\overline{\tau}_d = J^{\mathrm{T}}(q)\tau_d$, $\overline{B} = \frac{1}{r}\left[\begin{smallmatrix} 1 & 1 \\ b & -b \end{smallmatrix}\right]$.

However, it should be noted that due to the existence of measurement errors, load variation and unmodeled dynamics, obtaining the accurate model of the system in many cases is very difficult. Then considering the influence of the uncertain factors, the actual system dynamic model can be formulated as

$$(M_0 + \Delta M)\dot{u} + \overline{F} + \overline{\tau}_d = (B_0 + \Delta B)\tau, \tag{4}$$

where $M_0 + \Delta M = \overline{M}$, $B_0 + \Delta B = \overline{B}$, M_0 and B_0 are the nominal parts, ΔM and ΔB are the uncertain parts.

Define $f = [\, f_1 \ f_2 \,]^{\mathrm{T}} = M_0^{-1}[\Delta M\dot{u} + \overline{F} + \overline{\tau}_d - \Delta B\tau]$ is the system's lumped disturbance vector and $\psi = [\, \psi_1 \ \psi_2 \,]^{\mathrm{T}} = M_0^{-1}B_0\tau$ is the new control input vector. Then the system (4) can be further expressed as

$$\dot{u} + f = \psi. \tag{5}$$

Let the reference trajectory $q_r = [\, x_r \ y_r \ \theta_r \,]^{\mathrm{T}}$ generate by a virtual robot, which is described as

$$\begin{cases} \dot{x}_r = v_r \cos\theta_r, \\ \dot{y}_r = v_r \sin\theta_r, \\ \dot{\theta}_r = \omega_r, \end{cases} \tag{6}$$

where x_r and y_r are the Cartesian coordinates of its reference point; θ_r is the orientation; v_r and ω_r are the desired linear velocity and angular velocity, respectively.

Assumption 2.1 There exists an unknown positive constant L such that the absolute values of f_1, f_2, $\dot{f}_1$, and $\dot{f}_2$ are bounded by L.

The control objective is to design a robust finite-time tracking controller for the mobile robot with parametric uncertainties and disturbances such that the tracking errors can converge to zero within finite time.

3 Design of Nonlinear Extended State Observer

3.1 Nonlinear Extended State Observer Design

Although it's difficult for the system to accurately measure the lumped disturbance vector f in practice, but its estimated value can be obtained quickly by nonlinear extended state observer (NESO). In order to realize the estimation for the lumped disturbance vector f, we need to employ a new extended state vector $[\, x_{12} \ x_{22} \,]^{\mathrm{T}}$ and define $x_{11}{=}v$, $x_{21}{=}\omega$. Therefore, the equivalent system of (5) can be expressed as

$$\begin{cases} \dot{x}_{11} = x_{12} + \psi_1, \\ \dot{x}_{12} = h_1, \\ \dot{x}_{21} = x_{22} + \psi_2, \\ \dot{x}_{22} = h_2, \end{cases} \tag{7}$$

where h_j $(j = 1, 2)$ is the change rate of the lumped disturbance f_j $(j = 1, 2)$, i.e., $h_j = \dot{f}_j$, and h_j are assumed to be unknown but bounded functions.

Based on its design theory, the NESO of the system (7) is designed as

$$\begin{cases} e_1 = z_{11} - x_{11}, \\ \dot{z}_{11} = z_{12} - \beta_{11}\text{fal}(e_1, 0.5, \sigma) + \psi_1, \\ \dot{z}_{12} = -\beta_{12}\text{fal}(e_1, 0.25, \sigma), \\ e_2 = z_{21} - x_{21}, \\ \dot{z}_{21} = z_{22} - \beta_{21}\text{fal}(e_2, 0.5, \sigma) + \psi_2, \\ \dot{z}_{22} = -\beta_{22}\text{fal}(e_2, 0.25, \sigma), \end{cases} \tag{8}$$

where z_{1j}, z_{2j} are the observer values of the states x_{1j}, x_{2j} in the system (7), β_{1j}, β_{2j} $(j = 1, 2)$ denote the observer gains and the nonlinear function $\text{fal}(\cdot)$ has the following form[16, 17]

$$\text{fal}(e_j, \alpha_j, \sigma) = \begin{cases} |e_j|^{\alpha_j}\text{sign}(e_j), & |e_j| > \sigma, \\ e_j/\sigma^{1-\alpha_j}, & |e_j| \le \sigma, \end{cases} \tag{9}$$

where $\sigma > 0$ and $\alpha_1 = 0.5$, $\alpha_2 = 0.25$.

Remark 3.1 The lumped disturbances f_j $(j = 1, 2)$ and their time derivatives are bounded, in the practical system this assumption is reasonable. For instance, the unknown ground friction is always bounded, or the external disturbance and parametric uncertainties of the system are also limited in a practical application. In addition, the assumption is a basic precondition for the design of the NESO, which has been widely employed in [18, 19].

Remark 3.2 As pointed out in [18], if the observer parameters β_{1j}, β_{2j} are appropriately chosen the observer errors can converge to a domain of a small positive constant, that is $|x_{12} - z_{12}| \le l_1$, $|x_{22} - z_{22}| \le l_2$, where l_1 and l_2 are small positive constants.

3.2 Coefficients Determination of NESO via Pole Placement

From (8), we can see that in order to achieve satisfactory observation performance, the coefficients β_{1j}, β_{2j} should be tuned carefully through experience. In this section, we will employ pole placement technique[19] to determine the coefficients.

Define the state observer errors $\Delta_{1j} = z_{1j} - x_{1j}$, $\Delta_{2j} = z_{2j} - x_{2j}$, then according to (7) and (8), the dynamic of the state observer errors is obtained as

$$\begin{cases} \dot{\Delta}_{11} = \Delta_{12} - \beta_{11}\text{fal}(e_1, 0.25, \sigma), \\ \dot{\Delta}_{12} = -\beta_{12}\text{fal}(e_1, 0.5, \sigma) - h_1, \\ \dot{\Delta}_{21} = \Delta_{22} - \beta_{21}\text{fal}(e_2, 0.25, \sigma), \\ \dot{\Delta}_{22} = -\beta_{22}\text{fal}(e_2, 0.5, \sigma) - h_2. \end{cases} \tag{10}$$

Due to h_j $(j = 1, 2)$ are bounded, the nonlinear function $\text{fal}(\cdot)$ is smooth, and $\text{fal}(0, 0.25, \sigma) = 0$, $\text{fal}(0, 0.5, \sigma) = 0$, $\text{fal}'(\cdot) = \frac{d\text{fal}(\cdot)}{d\Delta_{11}} \neq 0$, $\text{fal}'(\cdot) = \frac{d\text{fal}(\cdot)}{d\Delta_{21}} \neq 0$, then by the Taylor formula (10)

can be rewritten as follows

$$\begin{cases} \dot{\Delta}_{11} = \Delta_{12} - \beta_{11}\mathrm{fal}'(e_1, 0.25, \sigma)\Delta_{11}, \\ \dot{\Delta}_{12} = -\beta_{12}\mathrm{fal}'(e_1, 0.5, \sigma)\Delta_{11} - h_1, \\ \dot{\Delta}_{21} = \Delta_{22} - \beta_{21}\mathrm{fal}'(e_2, 0.25, \sigma)\Delta_{21}, \\ \dot{\Delta}_{22} = -\beta_{22}\mathrm{fal}'(e_2, 0.5, \sigma)\Delta_{21} - h_2. \end{cases} \tag{11}$$

Define $\beta_{ij} = \frac{l_{ij}}{\mathrm{fal}'(\cdot)}$ $(i = 1, 2, j = 1, 2)$, we can get the following state space form

$$\dot{\Delta} = \widetilde{A}\Delta + \widetilde{B}h_j, \tag{12}$$

where

$$\widetilde{A} = \begin{bmatrix} -l_{i1} & 1 \\ -l_{i2} & 0 \end{bmatrix}, \quad \widetilde{B} = \begin{bmatrix} 0 \\ -1 \end{bmatrix}, \quad \Delta = \begin{bmatrix} \Delta_{i1} \\ \Delta_{i2} \end{bmatrix}.$$

From (12), we know that the determination of the parameters β_{ij} can be realized by the determination of the parameters l_{ij}. If we choose the desired pole p_i for the system (12), then the parameters l_{ij} can be obtained by (13).

$$\left|sI - \widetilde{A}\right| = \prod_{i=1}^{2}(s - p_i), \tag{13}$$

where s denotes the system pole; I is the identity matrix.

Remark 3.3 If there is no the second item on the right of (12), we can easily conclude that the estimated errors will asymptotically converge to zero by choosing the appropriate parameters l_{ij}. However, as pointed out in [20], although there exist h_j in (12) the estimated errors are bounded under the assumption that h_j are bounded, and the upper bounds are related to the bandwidth of the observer.

4 Controller Design and Stability Analysis

In this section, a finite-time trajectory tracking controller based on NESO is designed to improve the tracking performance of the mobile robot, and the stability analysis is also given. Firstly, for the controller design, a definition and some lemmas are given to show the stability of the system.

Definition 4.1 (see [21, 22]) A continuous vector field function $f(x) = (f_1(x), f_2(x), \cdots, f_n(x))^{\mathrm{T}}$ is said to be homogeneous of degree $k \in R$ and $k \geq -\max\{r_i,\ i = 1, 2, \cdots, n\}$ with respect to $\{r_1, r_2, \cdots, r_n\}$, where $r_i > 0$, if for any given $\varepsilon > 0$, we have

$$f_i(\varepsilon^{r_1}x_1, \varepsilon^{r_2}x_2, \cdots, \varepsilon^{r_n}x_n) = \varepsilon^{k+r_i}f_i(x_1, x_2, \cdots, x_n), \quad x \in R^n,\ i = 1, 2, \cdots, n. \tag{14}$$

The system $\dot{x} = f(x)$ is homogeneous if $f(x)$ is homogeneous.

Lemma 4.2 (see [23]) *Consider the following system*

$$\dot{x} = f(x) + \widehat{f}(x), \quad f(0) = 0, \quad x \in R^n, \tag{15}$$

where $f(x)$ is a continuous homogeneous vector field of degree $k < 0$ with respect to $(r_1, r_2, \cdots, r_n)$ and $\widehat{f}(x)$ satisfies $\widehat{f}(0) = 0$. Assume $x = 0$ is an asymptotically stable equilibrium of the system $\dot{x} = f(x)$. Then, $x = 0$ is a locally finite-time stable equilibrium of the system if $\lim_{\varepsilon \to 0} \frac{\widehat{f}_i(\varepsilon^{r_1} x_1, \varepsilon^{r_2} x_2, \cdots, \varepsilon^{r_n} x_n)}{\varepsilon^{k + r_i}} = 0,\ i = 1, 2, \cdots, n, \forall x \neq 0$.

Lemma 4.3 (see [24]) *Suppose a_1, a_2, $\cdots$, a_n and $0 < \varsigma < 2$ are all positive constants, then the following inequality holds:*

$$(a_1^2 + a_2^2 + \cdots + a_n^2)^{\varsigma} \leqslant (a_1^{\varsigma} + a_2^{\varsigma} + \cdots + a_n^{\varsigma})^2. \tag{16}$$

Lemma 4.4 (see [25]) *Suppose that a continuous, positive-definite function $V(t)$ satisfies the following inequality:*

$$\dot{V}(t) + \gamma V^{\mu}(t) \leq 0, \quad \forall t \geq t_0,\ V(t_0) \geq 0, \tag{17}$$

where $\gamma > 0$, $0 < \mu < 1$ are constants. Then for any given t_0, $V(t)$ satisfies the following inequality:

$$V^{1-\mu}(t) \leq V^{1-\mu}(t_0) - \gamma(1-\mu)(t - t_0), \qquad t_0 \leq t \leq t_1, \tag{18}$$

and $V(t) \equiv 0$ for $\forall t \geq t_1$ with $t_1 = t_0 + \frac{V^{1-\mu}(t_0)}{\gamma(1-\mu)}$.

4.1 Finite-Time Virtual Velocity Controller Design Based on Kinematic Model

In this subsection our objective is to design the virtual velocity controller v_c and ω_c to track the given trajectory as (6) within finite time.

Define the tracking error vector relative to the local coordinate frame Xm-Om-Ym which is fixed on the mobile robot as Figure 1.

$$\overline{E} = \begin{bmatrix} e_x & e_y & e_\theta \end{bmatrix}^{\mathrm{T}} = \begin{bmatrix} \cos\theta & \sin\theta & 0 \\ -\sin\theta & \cos\theta & 0 \\ 0 & 0 & 1 \end{bmatrix} \begin{bmatrix} x_r - x \\ y_r - y \\ \theta_r - \theta \end{bmatrix}. \tag{19}$$

Differentiate (19) along with (1) and we have

$$\dot{\overline{E}} = \begin{bmatrix} \dot{e}_x & \dot{e}_y & \dot{e}_\theta \end{bmatrix}^{\mathrm{T}} = \begin{cases} \omega_c e_y - v_c + v_r \cos e_\theta, \\ -\omega_c e_x + v_r \sin e_\theta, \\ \omega_r - \omega_c. \end{cases} \tag{20}$$

By analyzing the structure of (20), the virtual velocity control laws can be designed in two steps. Firstly, we design ω_c such that e_θ can converge to zero in finite time. Secondly, we design v_c to make the errors e_x and e_y converge to zero in finite time.

Firstly, the virtual angular velocity control law is designed as follows

$$\omega_c = \omega_r + k_1 |e_\theta|^{\beta_1} \mathrm{sign}(e_\theta), \tag{21}$$

where controller parameters $k_1 > 0$, $0 < \beta_1 < 1$.

Choose the following Lyapunov function

$$V_1 = \frac{1}{2}e_\theta^2. \tag{22}$$

Differentiating (22) along with (20) and (21), we have

$$\begin{aligned}\dot{V}_1 &= e_\theta \dot{e}_\theta \\ &= -e_\theta k_1 |e_\theta|^{\beta_1} \text{sign}(e_\theta) \\ &= -k_1 |e_\theta|^{\beta_1+1} \\ &= -2^{\frac{\beta_1+1}{2}} k_1 V_1^{\frac{\beta_1+1}{2}}.\end{aligned} \tag{23}$$

According to Lemma 4.4, it can be concluded that θ_e can converge to zero in finite time $t_\theta = t_0 + \frac{2V_1^{\frac{1-\beta_1}{2}}(t_0)}{k_1(1-\beta_1)2^{\frac{1+\beta_1}{2}}}$.

Secondly, based on the design of ω_c, we will design the control law of v_c, which will drive the errors e_x and e_y converge to zero in finite time after $t > t_\theta$. When $t > t_\theta$, $\omega_c = \omega_r$, the system (20) can be transformed into the following form

$$\begin{cases} \dot{e}_x = \omega_r e_y - v_c + v_r, \\ \dot{e}_y = -\omega_r e_x. \end{cases} \tag{24}$$

Therefore, the virtual linear velocity control law can be designed as follows

$$v_c = v_r + k_2 |e_x|^{\beta_2} \text{sign}(e_x) - k_3 \omega_r |e_y|^{\beta_3} \text{sign}(e_y), \tag{25}$$

where $k_2,\ k_3 > 0$, $0 < \beta_2,\ \beta_3 < 1$.

Then, the closed-loop system of (24) is

$$\begin{cases} \dot{e}_x = \omega_r e_y - k_2 |e_x|^{\beta_2} \text{sign}(e_x) + k_3 \omega_r |e_y|^{\beta_3} \text{sign}(e_y), \\ \dot{e}_y = -\omega_r e_x. \end{cases} \tag{26}$$

Choose the following Lyapunov function

$$V_2 = \frac{1}{2}e_x^2 + \frac{1}{2}e_y^2 + \frac{k_3}{1+\beta_3}|e_y|^{1+\beta_3}. \tag{27}$$

Differentiating (27) along with (24), we have

$$\begin{aligned}\dot{V}_2 &= e_x \dot{e}_x + e_y \dot{e}_y + k_3 |e_y|^{\beta_3} \dot{e}_y \text{sign}(e_y) \\ &= e_x(\omega_r e_y - k_2 |e_x|^{\beta_2} \text{sign}(e_x) + k_3 \omega_r |e_y|^{\beta_3} \text{sign}(e_y)) - e_y \omega_r e_x + k_3 |e_y|^{\beta_3} \dot{e}_y \text{sign}(e_y) \\ &= -k_2 |e_x|^{\beta_2+1} \\ &\le 0.\end{aligned} \tag{28}$$

Then, it can be concluded that the states e_x and e_y can converge to zero asymptotically. Global finite-time stability can be obtained if a system satisfies both global asymptotical stability and local finite-time stability[22].

In the following, we will prove the states e_x and e_y are local finite-time convergence.

System (26) can be divided into two parts

$$\begin{bmatrix} \dot{e}_x \\ \dot{e}_y \end{bmatrix} = g(e_x, e_y) + \widehat{g}(e_x, e_y), \tag{29}$$

where

$$g(e_x, e_y) = \begin{bmatrix} -k_2|e_x|^{\beta_2}\mathrm{sign}(e_x) + k_3\omega_r|e_y|^{\beta_3}\mathrm{sign}(e_y) \\ -\omega_r e_x \end{bmatrix},$$

$$\widehat{g}(e_x, e_y) = \begin{bmatrix} \widehat{g}_1(e_x, e_y) \\ \widehat{g}_2(e_x, e_y) \end{bmatrix} = \begin{bmatrix} \omega_r e_y \\ 0 \end{bmatrix}.$$

Consider the following system

$$\begin{bmatrix} \dot{e}_x \\ \dot{e}_y \end{bmatrix} = g(e_x, e_y). \tag{30}$$

Choose the following Lyapunov function

$$V_3 = \frac{1}{2}e_x^2 + \frac{k_3}{1+\beta_3}|e_y|^{1+\beta_3}. \tag{31}$$

Differentiating (31) along with (26), we have

$$\begin{aligned} \dot{V}_3 &= e_x\dot{e}_x + k_3|e_y|^{\beta_3}\mathrm{sign}(e_y)\dot{e}_y \\ &= -k_2|e_x|^{\beta_2+1} + k_3\omega_r e_x|e_y|^{\beta_3}\mathrm{sign}(e_y) - \omega_r e_x k_3|e_y|^{\beta_3}\mathrm{sign}(e_y) \\ &= -k_2|e_x|^{\beta_2+1} \le 0. \end{aligned} \tag{32}$$

Then, based on Lyapunov stability theory, $(e_x, e_y) = (0, 0)$ is an asymptotically stable equilibrium point of the system (26). If we choose $\beta_2 = \frac{2\beta_3}{1+\beta_3}$, it's easy to obtain that $g(e_x, e_y)$ with variables (e_x, e_y) is homogeneous of degree $k = \frac{\beta_3-1}{\beta_3+1}$ with respect to $(1, \frac{2}{\beta_3+1})$.

As for $\widehat{g}(e_x, e_y)$, we have

$$\lim_{\varepsilon\to 0}\frac{\widehat{g}_i(\varepsilon^{r_1}e_x, \varepsilon^{r_2}e_y)}{\varepsilon^{k+r_i}} = 0, \quad i = 1, 2, \ \ \forall (e_x, e_y) \neq 0, \tag{33}$$

where $r_1 = 1$, $r_2 = \frac{2}{1+\beta_3}$. According to Lemma 4.2, System (26) is locally finite-time stable. Thus, we can conclude that the system (20) is globally finite-time stable under the virtual velocity control laws of (21) and (25).

4.2 Finite-Time Tracking Control Based on Dynamic Model

Define the tracking error between virtual velocity vector $u_c = [\, v_c \ \omega_c \,]^{\mathrm{T}}$ and actual velocity vector $u = [\, v \ \omega \,]^{\mathrm{T}}$ as

$$E = u - u_c. \tag{34}$$

Then, the first-order derivative of the tracking error is given by

$$\dot{E} = \dot{u} - \dot{u}_c. \tag{35}$$

In order to ensure the states of the system converge to the equilibrium point quickly, we select the following fast terminal sliding mode surface

$$S = \begin{bmatrix} s_1 & s_2 \end{bmatrix}^{\mathrm{T}} = E + \int_0^t K_1 E + K_2 E^{q/p} dt, \tag{36}$$

where p, q are odd number, and selected to satisfy $q < p < 2q$; $K_1 = \left[\begin{smallmatrix} k_{11} & 0 \\ 0 & k_{12} \end{smallmatrix}\right] > 0$, $K_2 = \left[\begin{smallmatrix} k_{21} & 0 \\ 0 & k_{22} \end{smallmatrix}\right] > 0$ are the diagonal matrix.

Differentiating (36) with respect to time yields

$$\dot{S} = \dot{E} + K_1 E + K_2 E^{q/p}. \tag{37}$$

From (5) and (35), the equation (37) can be rewritten as

$$\dot{S} = \psi - f - \dot{u}_c + K_1 E + K_2 E^{q/p}. \tag{38}$$

Then, actual finite-time control law based on NESO can be designed as

$$\psi = \dot{u}_c - (K_1 E + K_2 E^{q/p}) + \begin{bmatrix} z_{12} \\ z_{22} \end{bmatrix} - K_3 |S|^{\beta_4} \mathrm{sign}(S), \tag{39}$$

where $|S|^{\beta_4}\mathrm{sign}(S) = \left[\, |s_1|^{\beta_4}\mathrm{sign}(s_1),\ |s_2|^{\beta_4}\mathrm{sign}(s_2) \,\right]^{\mathrm{T}}$, z_{12} and z_{22} are the observing values of the lumped disturbances f_1 and f_2, respectively, and $K_3 = \left[\begin{smallmatrix} k_{31} & 0 \\ 0 & k_{32} \end{smallmatrix}\right] > 0$ denotes the diagonal matrix.

Substituting (39) into (38), we can obtain the following equation

$$\dot{S} = \begin{bmatrix} z_{12} \\ z_{22} \end{bmatrix} - f - K_3 |S|^{\beta_4} \mathrm{sign}(S). \tag{40}$$

4.3 Stability Analysis

Theorem 4.5 *Consider the velocity tracking error system* (34)*, the nonlinear extended state observer* (8)*, the fast terminal sliding mode surface* (36) *and the control law* (39)*, the fast terminal sliding mode surface S will converge to a small region of origin in finite time, and also the tracking error will be stabilized at a relatively small region of origin within a finite time by choosing the appropriate controller parameters.*

Proof The following Lyapunov function is considered

$$V_4 = \frac{1}{2} S^{\mathrm{T}} S. \tag{41}$$

Differentiating (41), and using (40) yields

$$\begin{aligned} \dot{V}_4 &= S^{\mathrm{T}} \dot{S} \\ &= S^{\mathrm{T}} \left(\begin{bmatrix} z_{12} \\ z_{22} \end{bmatrix} - f - K_3 |S|^{\beta_4} \mathrm{sign}(S) \right) \\ &\leqslant \sum_{i=1}^{2} l_i \, |s_i| - \sum_{i=1}^{2} k_{3i} |s_i|^{\beta_4 + 1}. \end{aligned} \tag{42}$$

It is easy to find a positive constant η satisfied $\eta < \min\{k_{31}, k_{32}\}$. Thus, (42) can be rewritten as

$$\dot{V}_4 \leqslant - \sum_{i=1}^{2} (k_{3i} - \eta) |s_i|^{\beta_4 + 1} - \sum_{i=1}^{2} (\eta |s_i|^{\beta_4 + 1} - l_i \, |s_i|). \tag{43}$$

For (43), when $|s_i| > (\frac{l_i}{\eta})^{\frac{1}{\beta_4}}$, using Lemma 4.3, we have

$$\begin{aligned} \dot{V}_4 &\leqslant - \sum_{i=1}^{2} (k_{3i} - \eta) |s_i|^{\beta_4 + 1} \\ &\leqslant -\kappa \left(\sum_{i=1}^{2} |s_i|^2 \right)^{\frac{\beta_4 + 1}{2}} \\ &= -\kappa 2^{\frac{\beta_4 + 1}{2}} V_4^{\frac{\beta_4 + 1}{2}}, \end{aligned} \tag{44}$$

where $\kappa = \min\{k_{3i} - \eta\}$. According to Lemma 4.4, the region $|s_i| \leqslant (\frac{l_i}{\eta})^{\frac{1}{\beta_4}}$ can be reached in finite time, and by choosing the appropriate controller parameters it can be concluded that the sliding mode surface S can converge to a small region of origin in finite time. Furthermore, according to the finite time convergence feature of terminal sliding mode[26], we can obtain that the tracking error will be stabilized at a relatively small region of origin within a finite time. This completes the proof. ∎

5 Simulation

In this section the proposed control scheme FTC with NESO is applied to the wheeled mobile robot for verifying its effectiveness and superior performance. Besides, a finite time sliding mode controller (FTC) without NESO, and a robust tracking controller (RTC) in [27] are also given for the purpose of comparison.

As for the control scheme FTC without NESO, the corresponding sliding mode surface is designed as (36), the control law is designed as

$$\psi = \dot{u}_c - (K_1 E + K_2 E^{q/p}) - K_3 |S|^{\beta_4} \mathrm{sign}(S). \tag{45}$$

According to Reference [27], the expression of RTC is given as

$$\begin{cases} v_c = v_r \cos e_\theta + k_4 e_x, \\ \omega_c = \omega_r + k_5 v_r e_y + k_6 v_r \sin e_\theta, \end{cases} \tag{46}$$

$$\psi = \begin{bmatrix} z_{12} \\ z_{22} \end{bmatrix} - K_4 E, \tag{47}$$

where $k_4, k_5, k_6 > 0$ are the controller gains, and $K_4 = \left[\begin{smallmatrix} k_{41} & 0 \\ 0 & k_{42} \end{smallmatrix}\right] > 0$ is the diagonal matrix.

For fair comparison, the initial parameters of system and partial controller parameters are set as the same. The initial poses of the virtual robot and actual robot are $\left[\begin{smallmatrix} 0 & 0 & 0 \end{smallmatrix}\right]^{\mathrm{T}}$ and $\left[\begin{smallmatrix} 0.1 & 0.1 & \pi/8 \end{smallmatrix}\right]^{\mathrm{T}}$, respectively; the mobile robot parameters are set as $r = 0.05$ m, $b = 0.1$ m, $I = 2.7$ kg$\cdot$m^2, and $m = 4.5$ kg; the desired linear and angular velocities are set as $v_r = 1$ m/s and $\omega_r = 1$ rad/s; the auxiliary velocity controller parameters are set as $k_1 = 6$, $k_2 = 2$, $k_3 = 2$, $\beta_1 = 2/3$, and $\beta_2 = \beta_3 = 1/3$. The parameters of the FTC+NESO are designed as $l_{11} = l_{21} = 100$, $l_{12} = l_{22} = 6000$, $K_1 = \mathrm{diag}\{20,\ 20\}$, $K_2 = \mathrm{diag}\{15,\ 15\}$, $K_3 = \mathrm{diag}\{1,\ 1\}$, $q = 1$, $p = 1.5$, and $\beta_4 = 1/8$; the parameters of the control strategy FTC without NESO are designed as $K_1 = \mathrm{diag}\{20,\ 20\}$, $K_2 = \mathrm{diag}\{15,\ 15\}$, $K_3 = \mathrm{diag}\{8,\ 8\}$, $q = 1$, $p = 1.5$, and $\beta_4 = 1/8$; the parameters of the RTC are set as $k_4 = 2$, $k_5 = 10, k_6 = 22$, and $K_4 = \mathrm{diag}\{31,\ 40\}$.

The parameter uncertainties are chosen as $\Delta M = 0.01 M_o$, $\Delta B = 0.01 B_o$, and

$$\overline{\tau}_d = \begin{bmatrix} \sin(t) + 2.4 \\ \cos(t) + 2.5 \end{bmatrix} \mathrm{N} \cdot \mathrm{m}. \tag{48}$$

The simulation results are illustrated in Figures 2–5. Figure 2 is the estimation errors for the lumped disturbances. As shown in Figures 2(a) and (b), by selecting appropriate values of the observer gains, the estimation states z_{12} and z_{22} can converge to the actual disturbance values f_1 and f_2 in finite time, respectively. Figure 3 shows the trajectory tracking curves of three different schemes. Figure 3(a) shows the trajectory tracking curves of the proposed scheme, while the trajectory tracking curves of the other two schemes are shown in Figures 3(b) and (c), respectively.

Figure 4 shows the tracking errors of three different schemes with respect to time. From Figures 4(a) and (b), it is easy to see that the tracking errors and the response time of the proposed scheme are similar to those of FTC scheme. So the first two control schemes can all achieve fast convergence speed and very small steady errors, and the response time of tracking errors is about within 2 seconds. From Figures 4(a) and (c), we can seen that the tracking errors and the response time of the proposed scheme are all much better than those of the RTC in [27]. Figure 5 shows the control signals of three different schemes. In Figure 5, it can be seen that the control signals of FTC+NESO and RTC in [27] almost have no chattering, while the control signals of FTC have obvious chattering almost all the time. So through the comparison, we can conclude that the proposed scheme is more suitable to practically apply for WMR system than the other two control schemes.

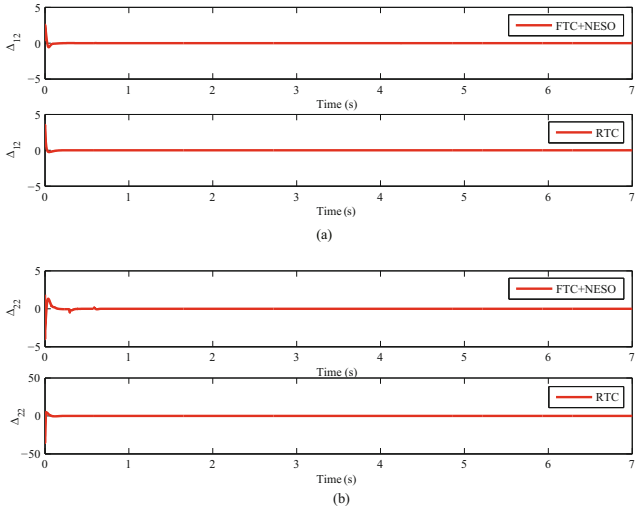

Figure 2 Estimation errors for lumped disturbances. (a) The estimation error of disturbance f_1. (b) The estimation error of disturbance f_2

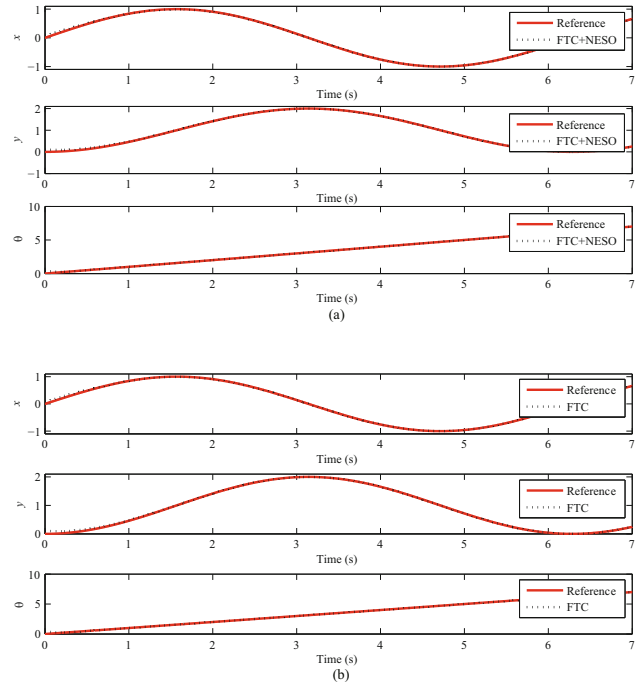

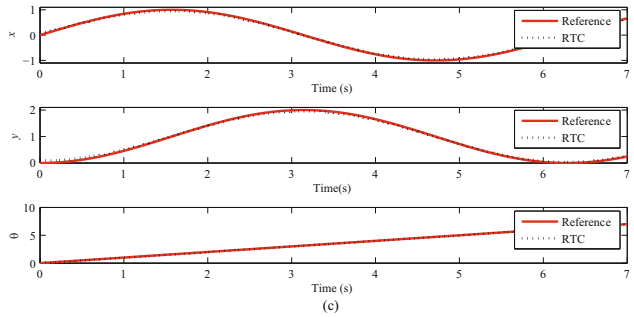

Figure 3 The trajectory tracking curves of three different schemes. (a) The trajectory tracking of FTC+NESO. (b) The trajectory tracking of FTC. (c) The trajectory tracking of RTC

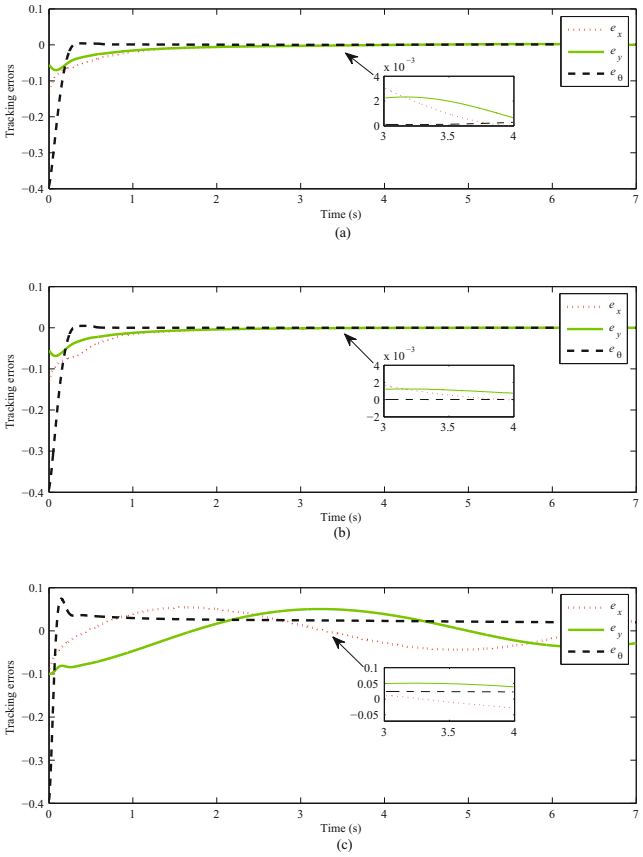

Figure 4 The tracking errors of three different schemes. (a) The tracking errors of FTC+NESO. (b) The tracking errors of FTC. (c) The tracking errors of RTC

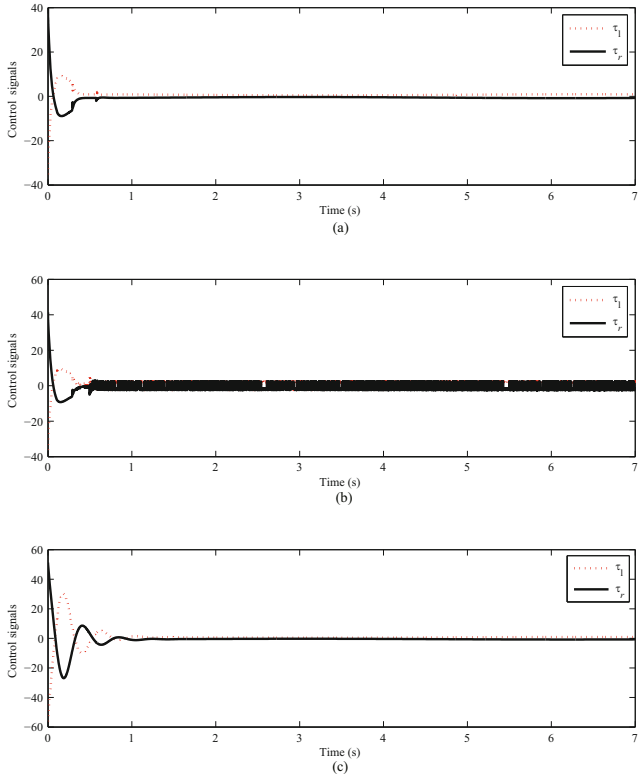

Figure 5 The control signals of three different schemes. (a) The control signals of FTC+NESO. (b) The control signals of FTC. (c) The control signals of RTC

6 Conclusions

In this paper, the trajectory tracking problem of WMR with lumped disturbances has been studied. By using NESO the lumped disturbances of the system can be successfully estimated, based on which a novel robust finite-time sliding mode controller has been developed. Detailed simulation results demonstrate that the proposed scheme can achieve a good control performance and the chattering phenomenon in the traditional finite-time sliding mode control can be obviously reduced.

References

[1] Fukao T, Nakagawa H, and Adachi N, Adaptive tracking control of a nonholonomic mobile robot, *IEEE Transactions on Robotics & Automation*, 2000, **16**(5): 609–615.

[2] Koubaa Y, Boukattaya M, and Dammak T, An adaptive control for uncertain mobile robot con-

sidering skidding and slipping effects, *proceedings of the* 5*th International Conference on Systems and Control*, Fac Sci Semlalia, Marrakech, MOROCCO, 2016, 13–19.

[3] Mahmood A O and Abdul R H, Robust backstepping tracking control of mobile robot based on nonlinear disturbance observer, *International Journal of Electrical and Computer Engineering*, 2016, **6**(2): 901–908.

[4] Dong W, Huo W, Tso S K, et al., Tracking control of uncertain dynamic nonholonomic system and its application to wheeled mobile robots, *IEEE Transactions on Robotics & Automation*, 2000, **16**(6): 870–874.

[5] Xu J X, Guo Z Q, and Tong H L, Design and implementation of integral sliding-mode control on an underactuated two-wheeled mobile robot, *IEEE Transactions on Industrial Electronics*, 2014, **61**(7): 3671–3681.

[6] Cui M, Liu W, Liu H, et al., Extended state observer-based adaptive sliding mode control of differential-driving mobile robot with uncertainties, *Nonlinear Dynamics*, 2016, **83**(2): 667–683.

[7] Tan L C, Bui T H, Tan T N, et al., Sliding mode control of two-wheeled welding mobile robot for tracking smooth curved welding path, *Journal of Mechanical Science and Technology*, 2004, **18**(7): 1094–1106.

[8] Li S, Wu C, and Sun Z, Design and implementation of clutch control for automotive transmissions using terminal-sliding-mode control and uncertainty observer, *IEEE Transactions on Vehicular Technology*, 2016, **65**(4): 1890–1898.

[9] Chen Q, Tang X Q, and Nan Y R, Finite-time neural funnel control for motor servo systems with unknown input constraint, *Journal of Systems Science and Complexity*, 2017, **30**(3): 579–594.

[10] Chen Q, Ren X, and Na J, Robust finite-time chaos synchronization of uncertain permanent magnet synchronous motors, *ISA Transactions*, 2015, **58**(3): 262–269.

[11] Xue W, Bai W, Yang S, et al., ADRC with adaptive extended state observer and its application to air-fuel ratio control in gasoline engines, *IEEE Transactions on Industrial Electronics*, 2015, **62**(9): 5847–5857.

[12] Wang J, Li S, Yang J, et al., Extended state observer-based sliding mode control for PWM-based DC-DC buck power converter systems with mismatched disturbances, *Control Theory & Applications Iet*, 2015, **9**(4): 579–586.

[13] Huang Y and Xue W C, Active disturbance rejection control: Methodology and theoretical analysis, *ISA Transactions*, 2014, **53**(4): 963–976.

[14] Talole S, Kolhe J, and Phadke S, Extended-state-observer-based control of flexible-joint system with experimental validation, *IEEE Transactions on Industrial Electronics*, 2010, **57**(4): 1411–1419.

[15] Zeng W, Wang Q, Liu F, et al., Learning from adaptive neural network output feedback control of a unicycle-type mobile robot, *ISA Transactions*, 2016, **61**(1): 337–347.

[16] Talole S E, Kolhe J P, and Phadke S B, Extended-state-observer-based control of flexible-joint system with experimental validation, *IEEE Transactions on Industrial Electronics*, 2010, **57**(4): 1411–1419.

[17] Xia Y, Zhu Z, and Fu M, Back-stepping sliding mode control for missile systems based on an extended state observer, *Control Theory & Applications IET*, 2011, **5**(1): 93–102.

[18] Han J Q, *Active Disturbance Rejection Control Technique — The Technique for Estimating and Compensating the Uncertainties*, National Defense Industry Press, Beijing, 2008.

[19] Kang Z J and Chen X Y, A design method of nonlinear extension state observer, *Electric Machines*

and Control, 2015, **5**(3): 199–203.

[20] Jiang Y, Sun Q, Zhang X, et al., Pressure regulation for oxygen mask based on active disturbance rejection control, *IEEE Transactions on Industrial Electronics*, 2017, **64**(8): 6402–6411.

[21] Bhat S P and Bernstein D S, Finite-time stability of homogeneous systems, *Proceedings of the American Control Conference*, University of Michigan, Ann Arbor, USA, 1997, 2513–2514.

[22] Ou M, Du H, and Li S, Finite-time formation control of multiple nonholonomic mobile robots, *International Journal of Robust & Nonlinear Control*, 2014, **24**(1): 140–165.

[23] Hong Y G, Xu Y S, and Huang J, Finite-time control for robot manipulators, *Systems and Control Letters*, 2002, **46**(4): 243–253.

[24] He S, Lin D, and Wang J, Autonomous spacecraft rendezvous with finite time convergence, *Journal of the Franklin Institute*, 2015, **352**(11): 4962–4979.

[25] Chen Q, Nan Y R, Zheng H H, et al., Full-order sliding mode control of uncertain chaos in a permanent magnet synchronous motor based on a fuzzy extended state observer, *Chinese Physics B*, 2015, **24**(11): 157–162.

[26] Wang F, Zong Q, and Tian B L, Finite time control design for re-entry hypersonic vehicle with disturbance observer, *Control Theory & Applications*, 2016, **33**(11): 1527–1534.

[27] Yang H, Fan X, Xia Y, et al., Robust tracking control for wheeled mobile robot based on extended state observer, *Advanced Robotics*, 2015, **30**(1): 68–78.